Elsevier Editorial System(tm) for Soil Biology and Biochemistry

Manuscript Draft

Manuscript Number: SBB12358R2

Title: Contributions of ryegrass, lignin and rhamnolipid to polycyclic aromatic hydrocarbon dissipation in an arable soil

Article Type: Research Paper

Keywords: Polycyclic aromatic hydrocarbons; Biostimulation; Rhizoremediation; Biosurfactant; Mineralization; Microbial community.

Corresponding Author: Professor Xiangui Lin,

Corresponding Author's Institution: Institute of Soil Science, Chinese Academy of Sciences

First Author: Yucheng Wu

Order of Authors: Yucheng Wu; Qingmin Ding; Qinghe Zhu; Jun Zeng; Rong Ji; Marc G Dumont, Dr.; Xiangui Lin

Manuscript Region of Origin: CHINA

Cover page

1. Type of contribution: Research paper

2. Data of preparation: 19 Nov, 2017

3. Number of text pages, tables and figures: 22 text pages, 2 tables and 6 figures

4. Title: Contributions of ryegrass, lignin and rhamnolipid to polycyclic aromatic hydrocarbon dissipation in an arable soil

5. Names of author:

Yucheng Wu [a,b], Qingmin Ding [a,b], Qinghe Zhu [a,b,c], Jun Zeng [a,b], Rong Ji [d], Marc G Dumont [e], Xiangui Lin [a,b,*]

6. Author affiliations

a Key Laboratory of Soil Environment and Pollution Remediation, Institute of Soil Science, Chinese Academy of Sciences, Nanjing 210008, China

b Joint Open Laboratory of Soil and the Environment, Hong Kong Baptist University & Institute of Soil Science, Chinese Academy of Sciences, Nanjing 210008, China

c University of Chinese Academy of Sciences, Beijing 100049, China

d State Key Laboratory of Pollution Control and Resource Reuse, School of the Environment, Nanjing University, Nanjing 210023, China

e Biological Sciences, University of Southampton, Southampton SO17 1BJ, U.K.

7. *Corresponding author:

Prof. Xiangui Lin
Key Laboratory of Soil Environment and Pollution Remediation
Institute of Soil Science, Chinese Academy of Sciences
Nanjing, 210008, P.R. China
Tel: +86 25 8688 1589; Fax: +86 25 8688 1000
E-mail: xglin@issas.ac.cn

* Corresponding author. Tel.: +86 25 8688 1589; Fax: +86 25 8688 1000; E-mail address: xglin@issas.ac.cn (X. Lin).

Abstract

Bioremediation of polycyclic aromatic hydrocarbon (PAH)-contaminated soil is often limited by inadequate microbial activity and/or low pollutant bioavailability. To explore the remediation potential of ryegrass and lignin, which are believed to improve microbial degradation, as well as the biosurfactant rhamnolipid, a pot experiment was performed with a long-term contaminated arable soil. A 41.7% reduction in 15 priority PAHs was achieved in the combined ryegrass, lignin and rhamnolipid treatment after 90 days. In contrast, there was no PAH reduction with any treatment used alone. The rhamnolipid was indispensable for successful remediation, as shown by the lack of PAH transformation in all non-rhamnolipid treatments. PAH in ryegrass biomass accounted for less than 0.1% of that detected in the initial soil, which, together with a theoretical estimation of plant transformation, suggested rhizoremediation rather than direct uptake contributed to PAH dissipation. High-throughput sequencing analysis demonstrated that lignin addition substantially changed the fungal and bacterial communities; however, there was no indication of lignin selection for known bacterial PAH degraders. Instead, a ^{14}C-spiked microcosm experiment showed that lignin amendment led to enhanced PAH mineralization and nonextractable residue formation. Taken together, these findings highlight the importance of simultaneous improvement of pollutant bioavailability and microbial activity for PAH bioremediation. A combination of rhizoremediation, biostimulation and surfactant appears to be promising in detoxifying long-term PAH-contaminated agricultural soil.

Key words

Polycyclic aromatic hydrocarbon; Biostimulation; Rhizoremediation; Biosurfactant; Mineralization; Microbial community.

1. Introduction

Polycyclic aromatic hydrocarbons (PAH) have two or more fused benzene rings and are predominantly formed during incomplete combustion of mineral fuels and biomass. The most recent estimate indicates that more than 520×10^3 tons of the 16 US Environment Protection Agency (USEPA) priority PAHs are released into the environment each year globally (Zhang and Tao, 2009), which may cause significant soil pollution through atmospheric deposition. PAHs are detected in soils around the world (Wilcke, 2007) and have been identified as major organic pollutants in agricultural soils of China (Lu et al., 2015). Thus, these chemicals pose potential human health risks via the food chain. As such, remediation measures should be taken for PAH-polluted agricultural soils.

Bioremediation is a promising approach to detoxifying PAH-contaminated soil through biological processes (Gan et al., 2009). Many bacteria can use PAHs as carbon and energy sources, resulting in their mineralization; however, PAHs with $\geqslant$4 rings (high molecular weight PAH, HMW PAH) are relatively resistant to bacterial degradation because of their high hydrophobicity and stability (Bamforth and Singleton, 2005). Compared to bacteria, fungi have different mechanisms for transforming PAHs, such as extracellular ligninolytic enzymes and intracellular cytochrome P450 monooxygenases (Harms et al., 2011), and mounting evidence suggests that fungi are a potential resource for the clean-up of HMW PAH-polluted soil (Aranda, 2016).

A series of strategies have been developed to enhance microbial degradation of PAH. Biostimulation, the addition of a bulking agent to stimulate soil microbes, is among the most common *in situ* treatments of agricultural soil. For example, successful reduction of HMW PAH was achieved by the addition of lignin-rich materials (Lladó et al., 2013), because ligninolytic enzymes,

such as LiP, MnP and laccase, have exceptional capacities for PAH transformation and may contribute to soil PAH dissipation through co-metabolic mechanisms (Wu et al., 2008b). Phytoremediation is another green technology for remediation of contaminated soil. Among others, ryegrass has a vast root system and has been widely used in bioremediation (Gan et al., 2009). Plants may enhance PAH dissipation by direct uptake (phytoextraction) or through rhizospheric processes (rhizoremediation) (Alkorta and Garbisu, 2001). Stimulation of rhizosphere microbes by root exudates tends to be the primary mechanism of rhizoremediation, as shown by a comprehensive analysis of rhizospheric microbial degraders (Bourceret et al., 2015). Nevertheless, the contribution of plant uptake has rarely been assessed (Gao and Zhu, 2004).

One crucial issue affecting biological transformation is the availability of pollutants. Surfactants are often used to increase the water solubility of hydrophobic organic pollutants, enhancing plant uptake (Zhu and Zhang, 2008) and improving microbial degradation (Fernando Bautista et al., 2009). Compared to synthetic surfactants that could be toxic to microorganisms, biosurfactants appear to be a safe alternative due to their biodegradability and biocompatibility (Ławniczak et al., 2013). Rhamnolipid is a biosurfactant produced by *Pseudomonas aeruginosa* and has shown potential in improving PAH bioavailability, thus is useful in the remediation of long-term aged contaminated soil (Mulligan, 2005).

In practice, remediation strategies are often combined for optimal pollutant removal. For example, surfactants coupled with biostimulation or phytoremediation combined with microbial inoculation are often more effective in remediation of aged polluted soil than any measure in isolation (Johnson et al., 2004; Lladó et al., 2015). In this study, we assessed the bioremediation of a long-term polluted arable soil using three strategies, namely phytoremediation (ryegrass),

67 biostimulation (lignin addition) and biosurfactant enhancement (rhamnolipid addition). Soil PAH
68 dissipation and plant uptake were monitored. Also, quantitative PCR and high-throughput
69 sequencing were used to detect shifts in the soil bacterial and fungal communities. A second
70 microcosm experiment was performed to examine the effects of lignin and rhamnolipid on freshly
71 spiked ^{14}C-benz(a)anthracene in the same arable soil. Both mineralization and soil fractionation of
72 the ^{14}C-PAH were determined. The aims of this study were therefore (1) to evaluate the combined
73 strategies in terms of soil detoxification, (2) to estimate the contributions of ryegrass, lignin and
74 rhamnolipid to PAH dissipation, and (3) to explore the mechanisms underlying the PAH dissipation.
75

76 **2. Materials and Methods**

77 *2.1. Soil*

78 The arable soil used in the study was collected on 7 Sep. 2015 near a smelting plant in Nanjing,
79 Jiangsu Province, China (31°53'48''N, 118°36'59''E). PAH pollution of agricultural soils around the
80 smelting plant has been previously reported (Wu et al., 2016a). At the time of sampling, the farmland
81 was used for maize cultivation. The soil was a sandy loam, with a pH of 7.1, 12.7 g kg^{-1} of total
82 carbon, 1.3 g kg^{-1} of total nitrogen, 0.57 g kg^{-1} of total phosphorus, and 19.3 g kg^{-1} of potassium (as
83 K_2O). The bulk density of the soil was 1.14 g cm^{-3}. The total amount of 15 USEPA priority PAHs
84 (excluding acenaphthylene) in this arable soil was 8.59 mg kg^{-1}, consisting of 11.0% 3-ring, 47.1%
85 4-ring, 28.7% 5-ring and 13.0% 6-ring PAH. Specifically, the concentration of benz(a)anthracene in
86 the soil was 0.85 mg kg^{-1}. The soil was air-dried, sieved (5 mm), homogenized and stored at room
87 temperature in the dark.

88 *2.2. Pot experiment*

For the pot experiment, 2.0 kg of air-dried soil was added to each plastic pot of 20-cm diameter, and the soil moisture was adjusted to 60% water holding capacity (WHC) at the beginning of the incubation. Seven treatments, including an unamended control, were established in four replicates as shown in Table 1. For each planted pot, 20 ryegrass (*Lolium multiflorum* Lam) plantlets from the germination of seeds on moist perlite for 7 days were transplanted. Alkali lignin (Sigma-Aldrich) was spiked into the soil at a concentration of 1% (w/w) and well mixed. Prior to the moisture adjustment on day 0 and 30, 125 ml of 2 g l^{-1} rhamnolipid (90% mixture of mono- and di-rhamnolipid, critical micelle concentration (CMC) 50 mg l^{-1}, Zijin Biotech, Huzhou, China) solution was slowly poured on the soil surface, giving a final concentration of 125 mg kg^{-1} soil. During the incubation, the pots were irrigated every 2-3 days to keep the soil moisture.

After a 90-day incubation in a greenhouse, a composite sample composed of five soil cores (approximately 15 cm in depth) was collected from each pot with an auger sampler. A 50-g subsample was stored at -20°C for molecular analysis, and the remaining sample was air-dried, sieved and stored at 4°C until PAH analysis. Ryegrass roots and shoots were separately harvested, rinsed, dried and homogenized prior to PAH determination.

2.3. PAH analysis

PAHs in soil and ryegrass were extracted and determined as previously described with minor modifications (Wu et al., 2016b). Briefly, 10.0 g of soil or 1.0 g of plant sample was spiked with 0.4 μg 1-fluoropyrene dissolved in acetone as an internal standard, and was extracted on a Soxhlet apparatus with dichloromethane for 24 h. Prior to the ultra-fast liquid chromatography (UFLC-20 system, Shimadzu, Kyoto, Japan) analysis, the extracts were concentrated and purified with activated silica gel. Fifteen of the 16 priority PAHs (excluding acenaphthylene) were determined with a

111 reversed phase C18 column (Shim-pack XR-ODSII, Kyoto, Japan). All concentrations are presented
112 based on a soil dry weight. The toxic equivalency factors (TEFs) of PAHs were obtained from the
113 literature (Nisbet and LaGoy, 1992).
114 *2.4. DNA extraction and quantitative PCR*
115 Soil DNA was extracted from about 0.5 g of sample with a FastDNA Spin Kit for Soil (MP
116 Biomedicals, OH) following the manufacturer's instructions. The quality and quantity of DNA were
117 assessed with a NanoDrop 1000 spectrophotometer (Thermo, DE) and by electrophoresis.
118 Tenfold-diluted DNA was used in all downstream analyses to avoid the inhibition of co-extracted soil
119 contaminants.
120 Bacterial 16S rRNA, fungal 18S rRNA and bacterial PAH-ring hydroxylating dioxygenase
121 (PAH-RHDα) genes were enumerated by quantitative PCR (qPCR) with the primer sets 515f/907r
122 (Stahl and Amann, 1991; Muyzer et al., 1995), nu-SSU-0817-5'/nu-SSU-1196-3' (Borneman and
123 Hartin, 2000) and GP-F/GP-R (Cébron et al., 2008), respectively. QPCR was performed on a CFX96
124 instrument (Bio-Rad) based on SYBR Green chemistry. Triplicate reactions were run for each sample,
125 and the qPCR was performed as described previously (Wu et al., 2015). All qPCR standards were
126 generated by cloning the respective gene fragments into the plasmid pEASY-T1 (Transgen Biotech,
127 Beijing, China). A dilution series of the standard plasmids across seven orders of magnitude (10^1
128 -10^7 copies μl^{-1}) was used. The control was always run with water as the template instead of DNA
129 extract. The qPCR amplification efficiency was 98.9% with an R^2-value of 0.994 for the bacterial
130 16S rRNA genes, 70.0% with an R^2-value of 0.998 for the fungal 18S rRNA genes, and 66.3% with
131 an R^2-value of 0.992 for the Gram-positive bacterial PAH-RHDα genes. Amplification specificity
132 was assessed by both melting curve analysis and electrophoresis.

133 *2.5. MiSeq sequencing of bacterial 16S and fungal 18S rRNA genes*

134 Soil bacterial and fungal communities were analysed on the Illumina MiSeq sequencing
135 platform. Briefly, the bacterial 16S rRNA and fungal 18S rRNA genes were amplified using the
136 primers described above, with the forward primers tagged with a 5-nucleotide (nt) barcode. After
137 verification by agarose gel electrophoresis, an equimolar mixture of PCR amplicons for each soil
138 sample was submitted for sequencing (Major Bio, Shanghai, China).

139 *2.6. Sequence processing and analysis*

140 Raw paired Illumina MiSeq reads were assembled and analysed using QIIME as described
141 previously (Chu et al., 2016). Reads with an average quality score of <25 were discarded.
142 Operational taxonomic units (OTUs) were assigned using UCLUST (Edgar, 2010) based on a
143 threshold of 97% sequence identity. The taxonomy of each representative of OTU was achieved by
144 alignment against the Greengenes rRNA gene database (http://greengenes.lbl.gov/). Nonmetric
145 multidimensional scaling (NMDS) analysis was performed with an OTU table using the vegan
146 package of R. A heatmap was generated with centered dominant phylotypes data using the R package
147 pheatmap version 1.0.8, with phylotypes and samples aggregated into clusters using the complete
148 neighbor method.

149 Co-occurrence patterns in bacterial and fungal communities were examined by network analysis
150 as previously described (Banerjee et al., 2016). Briefly, linear correlations between dominant OTUs
151 in each dataset, which comprised of four replicates from one treatment and four 0-day samples, were
152 calculated with the MINE software (Reshef et al., 2011). The calculation was based on the most
153 abundant 320 bacterial and 100 fungal OTUs, of which the relative abundances were > 0.05% of the
154 total sequences in each dataset. The networks were visualized in Cytoscape 3.5.1 (Shannon et al.,

155 2003) with only strong correlations shown ($r > 0.9$ or $r < -0.9$). Network topology parameters were
156 calculated using the NetworkAnalyzer tool implemented in Cytoscape.

157 The sequences obtained in this study were deposited in the NCBI Sequence Read Archive (SRA)
158 under the Accession no. PRJNA352451.

159 *2.7. ^{14}C-benzo(a)anthracene microcosm experiment*

160 The fate, including mineralization and distribution of [7,12-^{14}C]-benz(a)anthracene (American
161 Radiolabeled Chemicals, Inc., 10 mCi mmol^{-1}, dissolved in ethanol, radiochemical purity > 99%) in
162 this arable soil amended with lignin or rhamnolipid alone (treatments ^{14}C-L, ^{14}C-R), and with both
163 (^{14}C-LR) or neither (^{14}C-control) was examined in triplicate 15-ml Pyrex tubes. The amounts of
164 added lignin and rhamnolipid were same as the pot experiment.

165 Both ^{14}C- and unlabeled benz(a)anthracene (BaA) was spiked into the soil following a process
166 described previously (Wu et al., 2016b), giving the final radioactivity of 0.796 MBq kg^{-1} and
167 concentration of 100 mg kg^{-1}, respectively. After adjusting to 60% WHC, the tubes were closed with
168 stoppers equipped with alkali traps (1 ml of 1 M NaOH) and statically incubated at 25 °C for 12
169 weeks. The NaOH solution was periodically removed from the trap and the radioactivity was
170 measured with a liquid scintillation counter (Beckman-Coulter, USA) as described previously (Wang
171 et al., 2017b).

172 *2.8. Soil fractionation*

173 After the incubation, the soil from ^{14}C-BaA microcosms was freeze-dried and extracted with
174 60-ml dichloromethane (DCM) on a Soxhlet apparatus for 24 h. The extracts were evaporated and
175 dissolved in acetonitrile, and the radioactivity quantified by LSC was defined as a DCM extracted
176 fraction.

177 The nonextractable residues (NER) (Kästner et al., 2014) were further fractionated into fulvic
178 acids (FA), humic acids (HA), and humin following the method described by (Shan et al., 2011; Shan
179 et al., 2015). Briefly, the residual soil after DCM extraction was air-dried and was extracted with 0.1
180 M oxygen-free NaOH for 24 h by horizontal shaking. The alkaline extract was separated by
181 centrifugation at 11 000 g for 20 min, and was fractionated into FA and HA by acidification with 6 M
182 HCl. The alkaline-insoluble residues were defined as humin fraction. Radioactivities in the FA and
183 HA fractions were determined by LSC. The humin samples (approximately 0.5 g) were combusted at
184 900 °C for 4 min on a Biological Oxidizer (OX-500; Zinsser Analytic, Germany). The ^{14}C-labeled
185 CO_2 produced was absorbed with 15 ml of alkaline cocktail (Oxysolve C-400; Zinsser Analytic;
186 Germany) and counted by LSC.

187 *2.9. Statistics*

188 For multiple comparisons, one-way ANOVA and Tukey's *post hoc* test were carried out using
189 SPSS 13.0 (SPSS), with an α value of 0.05 selected for significance. Student's *t*-test was performed
190 to determine whether differences existed between groups.

191

192 **3. Results**

193 *3.1. Dissipation of PAH in the pot experiment*

194 After the 90-day remediation, the total amount of the 15 PAHs (ΣPAH) in the control pots was
195 unchanged compared to the initial value (Fig. 1A), indicating negligible natural attenuation. Ryegrass
196 (P), lignin (L) or rhamnolipid (R), when used separately, did not significantly change the PAH
197 concentrations. A combination of two or three of the measures promoted PAH dissipation, resulting
198 in 28.2±3.9% and 41.7±8.7% ΣPAH removal in the PR (ryegrass + rhamnolipid) and PLR (ryegrass

199 + lignin + rhamnolipid) treatments, respectively.

200 Transformation of individual PAH was related to their molecular weight. The dissipation of low
201 molecular weight PAH (LMW PAH), such as the 3-ring phenanthrene, anthracene, fluorene and
202 acenaphthene were generally stronger across all treatments (Fig. S1). PAHs with ⩾4 rings were more
203 recalcitrant, but the concentration of 4- and 5-ring PAHs decreased considerably in the combined
204 ryegrass and rhamnolipid treatments (PR and PLR). In PLR pots, 43.1±9.4% of 4-ring and 43.4±9.0%
205 of 5-ring PAHs were dissipated. The PAHs with TEF ⩾0.1 were considerably reduced in PR and
206 PLR compared to control pots (Fig. S2). In the case of benz(a)anthracene, the removal was 31.5±9.8
207 in PR and 55.3±13.6% in PLR, while use of lignin alone did not improve the dissipation (Fig. 1B).
208 Addition of lignin in PLR further enhanced the reduction of other HMW PAH including
209 benzo(b)fluoranthene, benzo(k)fluoranthene and benzo(a)pyrene (Fig. S2).

210 *3.2. PAH in the roots and shoots of ryegrass*

211 Lignin addition significantly decreased the biomass of both shoots and roots (Fig. 2A). PAH
212 concentrations in ryegrass biomass ranged from 348±36 to 504±45 μg kg^{-1} dry weight. In treatments
213 P and PL, shoot-PAH was significantly higher than the root-PAH, while in rhamnolipid added
214 treatments (PR and PLR) the PAH concentrations in shoots and roots were not significantly different
215 (Fig. 2B). The calculated ΣPAH in ryegrass shoots and roots per pot was between 2.22±0.83 μg in
216 the PLR treatment to 5.48±0.99 μg in the P treatment (Fig. 2C), which was below 0.1% of the PAH
217 in the 2-kg polluted soil.

218 Despite the dominance of HMW PAH (⩾4 ring) in the original soil, LMW PAH was the major
219 component in ryegrass shoots and comprised >60% of the total amount (Fig. 3), while 5- and 6-ring
220 PAHs were relatively less. In contrast, the roots had higher 5- and 6-ring fractions than the shoots.

221 Addition of rhamnolipid did not significantly change the PAH profile in the roots and shoots;
222 however, lignin caused an increase of the 5-ring fraction in the roots.

223 *3.3. Gene abundances*

224 Significant (p<0.01) treatment effects were observed on the abundance of bacterial 16S rRNA,
225 fungal 18S rRNA and GP PAH-RHDα genes after the 90-day remediation (Fig. 4). For the bacterial
226 16S rRNA genes, there were similar copy numbers in treatment P and control pots. Rhamnolipid
227 slightly enhanced the bacterial growth at a non-significant level, and a nearly two-fold increase was
228 observed in all lignin-treated samples (Fig. 4A). This pattern of lignin stimulation was also found
229 with the fungal 18S rRNA gene (Fig. 4B), although the copies were normally two orders of
230 magnitude lower than that of the bacterial counterpart. Despite a failure to detect the GN PAH-RHDα
231 gene, the GP PAH-RHDα gene was successfully amplified from all samples. There was no
232 relationship between PAH dissipation and PAH-RHDα gene abundance, as indicated by the similar
233 copies in PR- and PLR-treated soils with those in other treatments (Fig. 4C).

234 *3.4. Changes in bacterial and fungal communities*

235 The Illumina MiSeq sequencing generated 1.24 million bacterial 16S rRNA gene reads. After
236 quality control, 35,840 to 56,073 reads for each sample were obtained. The dominant phyla in the
237 soils were Proteobacteria, Acidobacteria, Actinobacteria, Chloroflexi and Bacteroidetes, of which the
238 relative abundances were consistently >5% across all treatments. An NMDS analysis revealed a clear
239 separation of treatments depending on the presence or absence of lignin (Fig. 5A), meanwhile the
240 effects of ryegrass and rhamnolipid on community composition were comparatively small. Changes
241 in relative abundance of the dominant bacterial phylotypes among the treatments were revealed by a
242 heatmap analysis (Fig. S3). Interestingly, the influence of lignin on dominant bacterial OTUs was

largely different across the treatments, although a few phylotypes affiliated with Xanthomonadales and Myxococcales were consistently enriched.

In total, 1.18 million eukaryotic 18S rRNA gene reads were generated, with 34,536-59,017 sequences obtained from each library. After removing non-fungal sequences, which varied from 5% to 20% of each library, most sequences clustered with Ascomycota, within which those from Sordariomycetes were the most abundant. The fungal communities of lignin-amended soils were distinct from those in the other treatments (Fig. 5B), albeit there were two outliers from the PL treatment. Some phylotypes within Ascomycota or Chytridiomycota were consistently enriched or diminished in all lignin-treated pots (Fig. S4). Ryegrass appeared to be beneficial to Glomeromycota, a potential plant symbiont.

The network analysis identified considerable changes in the co-occurrence patterns in response to the treatments. The networks of combined treatments (PL, PR and PLR) had more average neighbors and shorter characteristic path lengths than when used alone (P, L, R) or in the control (Table 2). In particular, ryegrass increased the number of edges connected to a few fungal nodes, for example the arbuscular mycorrhizal fungus *Diversispora* within Glomeromycota (Fig. S5).

3.5. Fate of BaA in artificially contaminated microcosms

In the arable soil, 5.43±0.98% of the spiked ^{14}C-BaA was mineralized at an almost constant rate over the 12 weeks in the ^{14}C-control microcosms (Fig. 6A). Addition of 1% lignin increased the final mineralization to 7.38±0.89% in ^{14}C-L microcosms. Rhamnolipid did not significantly stimulate $^{14}C\text{-}CO_2$ emission, but the highest mineralization was observed in the combined lignin and rhamnolipid treatment (7.62±0.05% in ^{14}C-LR). Indeed, mineralization in the rhamnolipid microcosms (^{14}C-R and ^{14}C-LR) was only slightly higher than in the respective non-rhamnolipid

265 microcosms (^{14}C-control and ^{14}C-L).

266 In addition to mineralization, the residual ^{14}C was fractionated into DCM extractable and
267 nonextractable residues (NER) (Fig. 6B). The DCM extract contained a major fraction of the spiked
268 radioactivity (47.9-57.8% across the four treatments), although the chemical species of the ^{14}C atoms
269 were unknown. Based on the solubility in alkaline and acidic solutions, the NER was further
270 fractionated into FA-, HA-, and humin-bound residues. The ^{14}C associated with FA represented a tiny
271 fraction (approximately 2%), which was 10-fold less than those bound to humin. There was no
272 significant difference between treatments for the FA and humin fractions; however, as observed for
273 the mineralization, addition of lignin significantly increased the radioactivity bound to HA in the
274 ^{14}C-L and ^{14}C-LR microcosms.

275

276 **4. Discussion**

277 *4.1. Enhanced PAH dissipation by simultaneous improvement of microbial degradation and pollutant*
278 *bioavailability*

279 The contaminated soil used in this study was collected from an agricultural plot near an iron
280 smelting plant, which has been in operation for more than 40 years. A previous study revealed wide
281 PAH contamination in agricultural soils around this smelting plant (Wu et al., 2016a). The total
282 amount of PAH before the remediation was much higher than that observed in agricultural soils from
283 the Yangtse Delta of China (Ping et al., 2007), and the 5-ring benzo(a)pyrene concentration was
284 7-fold higher than an agricultural soil quality standard (100 μg kg^{-1}) (CCME, 2008).

285 The PAH dissipation in the pot experiment after the 90-day incubation highlights the importance
286 of simultaneous enhancement of biological transformation and pollutant bioavailability. This became

more evident when ryegrass and lignin were included as a combined stimulating factor (PL) for soil microbes. Neither PL nor R treatment significantly enhanced PAH dissipation, while a combination of PL and R (treatment PLR) reduced PAH to a greater extent (Fig. 1). Indeed, surfactant is often indispensable for the remediation of long-term contaminated soils (Mulligan, 2005). Interestingly, in the ^{14}C microcosm experiment the CO_2 mineralized from BaA was only marginally promoted by the addition of rhamnolipid (compare ^{14}C-control to ^{14}C-R, and ^{14}C-L to ^{14}C-LR in Fig. 6A). It can be assumed that the freshly added BaA had high bioavailability, resulting in the similar mineralization rates between the treatments with or without rhamnolipid application.

On the other hand, the substantial changes in microbial communities in the PLR pots, as well as the increased $^{14}CO_2$ production in the lignin amended microcosms, suggest the PAH dissipation must have been related to microbial stimulation. Due to the lack of a lignin-rhamnolipid combination (treatment LR) in the pot experiment, the effects of ryegrass and lignin in the presence of rhamnolipid could not be compared. Nevertheless, the mechanisms underlying ryegrass and lignin enhanced PAH dissipation could be explored with further analyses.

4.2. Involvement of ryegrass in PAH dissipation

Plants enhance PAH dissipation through various mechanisms (Alagić et al., 2015). Despite the lack of information on PAH dynamics in ryegrass biomass during the remediation, the contribution of the uptake and subsequent accumulation or transformation in ryegrass to PAH dissipation appears to be small. For one thing, the PAH in ryegrass represented <0.1% of that in the original soil (Fig. 3), suggesting negligible phytoaccumulation. For another, PAH transformation within plants is normally slow and is insufficient to explain the PAH dissipation in the arable soil. For example, the fastest PAH transformation in tall fescue was 0.4 μg g^{-1} biomass d^{-1} (Gao et al., 2013), which corresponds to

309 an approximately 90 μg kg^{-1} decrease in planted pots after 90-day remediation assuming the same
310 transformation rate for ryegrass. Together with the translocation limits of HMW PAH in plants (Tao
311 et al., 2009), the PAH dissipation in this arable soil could be associated with processes independent
312 of the ryegrass uptake.

313 Instead, ryegrass can promote HMW PAH dissipation through rhizospheric processes
314 (Ortega-Calvo et al., 2013), including stimulation of microbes. Although the copies of ribosomal
315 RNA and PAH-RHDα genes remained stable (Fig. 4), the community changes and fungal network in
316 planted soil (Fig. 5, Fig. S5) suggest an impact of roots on indigenous microorganisms. This
317 influence was reflected in a general stimulation of rhizosphere microbes rather than an enrichment of
318 PAH degraders. More sensitive approaches, such as omic technologies (Oburger and Schmidt, 2016),
319 will facilitate a direct assessment of the PAH degradation activity of rhizosphere microbes.

320 *4.3. Possible mechanisms underlying lignin-assisted remediation*

321 Lignin, in conjunction with ryegrass and rhamnolipid, enhanced the dissipation of HMW PAH
322 (PLR in Fig. 1), particularly the highly toxic benzo(a)pyrene (Fig. S2). The overall ~50% decrease in
323 ΣPAH in PLR pots is extraordinary in light of the long pollution history of the site and of the
324 possible formation of PAH from lignin (Grice et al., 2009). The ^{14}C experiment offered a valuable
325 opportunity to probe the mechanisms underlying the lignin-enhanced PAH remediation (Fig. 6).
326 Firstly, as demonstrated by the increase in HA-bound ^{14}C in ^{14}C-L and ^{14}C-LR microcosms, lignin
327 enhances the formation of NER. This is related to the production of reactive intermediates through
328 chemical and biological processes (Wang et al., 2017a); however, the contribution of lignin-enhanced
329 NER formation to soil remediation in the pot experiment could be small because no significant BaA
330 dissipation was observed in the L treatment. On the other hand, 23.8% more BaA dissipation in PLR

than in PR pots suggests lignin is capable of stimulating microbial degradation of PAH (Fig. 1B). It should be noted that lignin is a complex polymer, and whether the production of aromatic intermediates during its decomposition (Bugg et al., 2011) stimulates microbial PAH degradation merits further study.

It is very likely that lignin contributes to the soil detoxification by modification of the microbial community. The fungal community was susceptible to lignin amendment, as exemplified by the enrichment of several Ascomycetes. Ascomycota are a useful resource for remediation of hazardous chemicals (Aranda, 2016), though very little information is available about PAH transformation by the enriched Ascomycetes in lignin-treated samples. Successful remediation of PAH-contaminated soil has been achieved by Ascomycete inoculation (Wu et al., 2008a) or by fungal stimulation using mushroom cultivation substrates (Li et al., 2012). An interesting observation is the preferential transformation of some HMW PAH by fungal P450 (Syed et al., 2013) or ligninolytic enzymes (Wu et al., 2008b), which is consistent with the increased transformation of 4- and 5-ring PAHs in the PLR compared to PR pots (Fig. S1). Insight into the comprehensive influence of lignin on soil fungi is helpful for elucidating the mechanisms underlying the lignin-assisted PAH dissipation.

Meanwhile, the increased abundances, community changes, as well as the enrichment of a few dominant taxa within Xanthomonadales and Myxococcales (Fig. S3) indicate a functional succession of soil bacteria in all treatments with lignin. Although there was no evidence indicating an increase in bacterial PAH degraders in PLR soil (Fig. 4C), this does not indicate that bacterial PAH transformation was not enhanced. More sensitive and convincing methods, such as transcriptional analyses (de Menezes et al., 2012) and stable isotope probing (Rodgers-Vieira et al., 2015), may provide new evidence of the relative contribution of bacteria and fungi to the remediation of

PAH-contaminated soil.

4.4. Rhamnolipid as a safe biosurfactant

One concern associated with surfactant application is its environmental impact. Some synthetic surfactants are toxic to functionally important bacteria (Brandt et al., 2001) or change bacterial community composition (Singleton et al., 2016). In contrast, rhamnolipid is a carbon source supporting bacterial growth in soil (Fig. 4A) (Mulligan, 2005); thus, it is biocompatible. Rhamnolipid is also biodegradable (Wen et al., 2009) and has a minimal influence on plant growth (Fig. 2A) and community succession (Fig. 5). Overall, these findings suggest that rhamnolipid is a safe biosurfactant in terms of its effects on plant biomass and indigenous microbial communities.

To summarize, the combination of ryegrass, lignin and rhamnolipid resulted in considerable PAH dissipation in an aged contaminated arable soil at laboratory scale. Ryegrass and lignin substantially altered microbial abundance, composition, and network structure, implicating their potential in stimulating microbial PAH degradation, which became evident in the presence of the biosurfactant rhamnolipid. Specifically, lignin contributed to soil detoxification by enhanced PAH mineralization and NER formation. Overall, these findings highlight the importance of simultaneous improvement of microbial activity and PAH bioavailability, which should be considered in field-scale bioremediation of PAH-contaminated soil.

Acknowledgements

We thank Junli Hu, Jun Shan, Yu Shi and Kunkun Fan for the helpful suggestions to the experiment design and data analysis. This work was supported by the National Natural Science

375 Foundation of China (41371310, 41671266), the 973 Programme of the Ministry of Science and
376 Technology of China (2014CB441106), and the State Key Laboratory of Soil and Sustainable
377 Agriculture (Y212000014).

378

379 **References**

380 Alagić, S.Č., Maluckov, B.S., Radojičić, V.B., 2015. How can plants manage polycyclic aromatic hydrocarbons? May
381 these effects represent a useful tool for an effective soil remediation? A review. Clean Technologies and
382 Environmental Policy 17, 597-614.

383 Alkorta, I., Garbisu, C., 2001. Phytoremediation of organic contaminants in soils. Bioresource Technology 79, 273-276.

384 Aranda, E., 2016. Promising approaches towards biotransformation of polycyclic aromatic hydrocarbons with
385 Ascomycota fungi. Current Opinion in Biotechnology 38, 1-8.

386 Bamforth, S.M., Singleton, I., 2005. Bioremediation of polycyclic aromatic hydrocarbons: current knowledge and future
387 directions. Journal of Chemical Technology & Biotechnology 80, 723-736.

388 Banerjee, S., Kirkby, C.A., Schmutter, D., Bissett, A., Kirkegaard, J.A., Richardson, A.E., 2016. Network analysis reveals
389 functional redundancy and keystone taxa amongst bacterial and fungal communities during organic matter
390 decomposition in an arable soil. Soil Biology and Biochemistry 97, 188-198.

391 Borneman, J., Hartin, R.J., 2000. PCR primers that amplify fungal rRNA genes from environmental samples. Applied
392 and Environmental Microbiology 66, 4356-4360.

393 Bourceret, A., Leyval, C., de Fouquet, C., Cébron, A., 2015. Mapping the centimeter-scale spatial variability of PAHs and
394 microbial populations in the rhizosphere of two plants. PLoS ONE 10, e0142851.

395 Brandt, K.K., Hesselso/e, M., Roslev, P., Henriksen, K., So/rensen, J., 2001. Toxic effects of linear alkylbenzene
396 sulfonate on metabolic activity, growth rate, and microcolony formation of *Nitrosomonas* and *Nitrosospira* Strains.
397 Appl Environ Microbiol 67, 2489-2498.

398 Bugg, T.D.H., Ahmad, M., Hardiman, E.M., Singh, R., 2011. The emerging role for bacteria in lignin degradation and
399 bio-product formation. Current Opinion in Biotechnology 22, 394-400.

400 Cébron, A., Norini, M.-P., Beguiristain, T., Leyval, C., 2008. Real-Time PCR quantification of PAH-ring hydroxylating
401 dioxygenase (PAH-RHDα) genes from Gram positive and Gram negative bacteria in soil and sediment samples.
402 Journal of Microbiological Methods 73, 148-159.

403 CCME, 2008. Canadian soil quality guidelines for carcinogenic and other polycyclic aromatic hydrocarbons
404 (environmental and human health effects), p. 218.

405 Chu, H., Sun, H., Tripathi, B.M., Adams, J.M., Huang, R., Zhang, Y., Shi, Y., 2016. Bacterial community dissimilarity
406 between the surface and subsurface soils equals horizontal differences over several kilometers in the western Tibetan
407 Plateau. Environmental Microbiology 18, 1523-1533.

de Menezes, A., Clipson, N., Doyle, E., 2012. Comparative metatranscriptomics reveals widespread community responses during phenanthrene degradation in soil. Environmental Microbiology 14, 2577-2588.

Edgar, R.C., 2010. Search and clustering orders of magnitude faster than BLAST. Bioinformatics 26, 2460-2461.

Fernando Bautista, L., Sanz, R., Carmen Molina, M., González, N., Sánchez, D., 2009. Effect of different non-ionic surfactants on the biodegradation of PAHs by diverse aerobic bacteria. International Biodeterioration & Biodegradation 63, 913-922.

Gan, S., Lau, E.V., Ng, H.K., 2009. Remediation of soils contaminated with polycyclic aromatic hydrocarbons (PAHs). Journal of Hazardous Materials 172, 532-549.

Gao, Y., Zhang, Y., Liu, J., Kong, H., 2013. Metabolism and subcellular distribution of anthracene in tall fescue (Festuca arundinacea Schreb.). Plant and Soil 365, 171-182.

Gao, Y., Zhu, L., 2004. Plant uptake, accumulation and translocation of phenanthrene and pyrene in soils. Chemosphere 55, 1169-1178.

Grice, K., Lu, H., Atahan, P., Asif, M., Hallmann, C., Greenwood, P., Maslen, E., Tulipani, S., Williford, K., Dodson, J., 2009. New insights into the origin of perylene in geological samples. Geochimica et Cosmochimica Acta 73, 6531-6543.

Harms, H., Schlosser, D., Wick, L.Y., 2011. Untapped potential: exploiting fungi in bioremediation of hazardous chemicals. Nat Rev Micro 9, 177-192.

Johnson, D.L., Maguire, K.L., Anderson, D.R., McGrath, S.P., 2004. Enhanced dissipation of chrysene in planted soil: the impact of a rhizobial inoculum. Soil Biology and Biochemistry 36, 33-38.

Kästner, M., Nowak, K.M., Miltner, A., Trapp, S., Schäffer, A., 2014. Classification and modelling of nonextractable residue (NER) formation of xenobiotics in soil – A synthesis. Critical Reviews in Environmental Science and Technology 44, 2107-2171.

Ławniczak, Ł., Marecik, R., Chrzanowski, Ł., 2013. Contributions of biosurfactants to natural or induced bioremediation. Applied Microbiology and Biotechnology 97, 2327-2339.

Li, X., Wu, Y., Lin, X., Zhang, J., Zeng, J., 2012. Dissipation of polycyclic aromatic hydrocarbons (PAHs) in soil microcosms amended with mushroom cultivation substrate. Soil Biology and Biochemistry 47, 191-197.

Lladó, S., Covino, S., Solanas, A.M., Petruccioli, M., D'annibale, A., Viñas, M., 2015. Pyrosequencing reveals the effect of mobilizing agents and lignocellulosic substrate amendment on microbial community composition in a real industrial PAH-polluted soil. Journal of Hazardous Materials 283, 35-43.

Lladó, S., Covino, S., Solanas, A.M., Viñas, M., Petruccioli, M., D'annibale, A., 2013. Comparative assessment of bioremediation approaches to highly recalcitrant PAH degradation in a real industrial polluted soil. Journal of Hazardous Materials 248–249, 407-414.

Lu, Y., Song, S., Wang, R., Liu, Z., Meng, J., Sweetman, A.J., Jenkins, A., Ferrier, R.C., Li, H., Luo, W., Wang, T., 2015. Impacts of soil and water pollution on food safety and health risks in China. Environment International 77, 5-15.

Mulligan, C.N., 2005. Environmental applications for biosurfactants. Environmental Pollution 133, 183-198.

Muyzer, G., Teske, A., Wirsen, C.O., Jannasch, H.W., 1995. Phylogenetic relationships of *Thiomicrospira* species and

444 their identification in deep-sea hydrothermal vent samples by denaturing gradient gel electrophoresis of 16S rDNA
445 fragments. Archives of Microbiology 164, 165-172.

446 Nisbet, I.C.T., LaGoy, P.K., 1992. Toxic equivalency factors (TEFs) for polycyclic aromatic hydrocarbons (PAHs).
447 Regulatory Toxicology and Pharmacology 16, 290-300.

448 Oburger, E., Schmidt, H., 2016. New methods to unravel rhizosphere processes. Trends in Plant Science 21, 243-255.

449 Ortega-Calvo, J.J., Tejeda-Agredano, M.C., Jimenez-Sanchez, C., Congiu, E., Sungthong, R., Niqui-Arroyo, J.L., Cantos,
450 M., 2013. Is it possible to increase bioavailability but not environmental risk of PAHs in bioremediation? Journal of
451 Hazardous Materials 261, 733-745.

452 Ping, L.F., Luo, Y.M., Zhang, H.B., Li, Q.B., Wu, L.H., 2007. Distribution of polycyclic aromatic hydrocarbons in thirty
453 typical soil profiles in the Yangtze River Delta region, east China. Environmental Pollution 147, 358-365.

454 Reshef, D.N., Reshef, Y.A., Finucane, H.K., Grossman, S.R., McVean, G., Turnbaugh, P.J., Lander, E.S., Mitzenmacher,
455 M., Sabeti, P.C., 2011. Detecting novel associations in large data sets. Science 334, 1518-1524.

456 Rodgers-Vieira, E.A., Zhang, Z., Adrion, A.C., Gold, A., Aitken, M.D., 2015. Identification of anthraquinone-degrading
457 bacteria in soil contaminated with polycyclic aromatic hydrocarbons. Appl Environ Microbiol 81, 3775-3781.

458 Shan, J., Ji, R., Yu, Y., Xie, Z., Yan, X., 2015. Biochar, activated carbon, and carbon nanotubes have different effects on
459 fate of (14)C-catechol and microbial community in soil. Scientific Reports 5, 16000.

460 Shan, J., Jiang, B., Yu, B., Li, C., Sun, Y., Guo, H., Wu, J., Klumpp, E., Schäffer, A., Ji, R., 2011. Isomer-Specific
461 Degradation of Branched and Linear 4-Nonylphenol Isomers in an Oxic Soil. Environmental Science & Technology
462 45, 8283-8289.

463 Shannon, P., Markiel, A., Ozier, O., Baliga, N.S., Wang, J.T., Ramage, D., Amin, N., Schwikowski, B., Ideker, T., 2003.
464 Cytoscape: a software environment for integrated models of biomolecular interaction networks. Genome Research
465 13, 2498-2504.

466 Singleton, D.R., Adrion, A.C., Aitken, M.D., 2016. Surfactant-induced bacterial community changes correlated with
467 increased polycyclic aromatic hydrocarbon degradation in contaminated soil. Applied Microbiology and
468 Biotechnology, 1-13.

469 Stahl, D.A., Amann, R., 1991. Development and application of nucleic acid probes, In: Stackebrandt, E., Goodfellow, M.
470 (Eds.), Nucleic Acid Techniques in Bacterial Systematics. Wiley, New York, pp. 205-248.

471 Syed, K., Porollo, A., Lam, Y.W., Grimmett, P.E., Yadav, J.S., 2013. CYP63A2, a catalytically versatile fungal P450
472 monooxygenase capable of oxidizing higher-molecular-weight polycyclic aromatic hydrocarbons, alkylphenols, and
473 alkanes. Appl Environ Microbiol 79, 2692-2702.

474 Tao, Y., Zhang, S., Zhu, Y.-g., Christie, P., 2009. Uptake and acropetal translocation of polycyclic aromatic hydrocarbons
475 by wheat (Triticum aestivum L.) grown in field-contaminated soil. Environmental Science & Technology 43,
476 3556-3560.

477 Wang, S., Sun, F., Wang, Y., Wang, L., Ma, Y., Kolvenbach, B.A., Corvini, P.F.-X., Ji, R., 2017a. Formation,
478 characterization, and mineralization of bound residues of tetrabromobisphenol A (TBBPA) in silty clay soil under
479 oxic conditions. Science of The Total Environment 599–600, 332-339.

480 Wang, Y., Xu, J., Shan, J., Ma, Y., Ji, R., 2017b. Fate of phenanthrene and mineralization of its non-extractable residues

481 in an oxic soil. Environmental Pollution 224, 377-383.

482 Wen, J., Stacey, S.P., McLaughlin, M.J., Kirby, J.K., 2009. Biodegradation of rhamnolipid, EDTA and citric acid in
483 cadmium and zinc contaminated soils. Soil Biology and Biochemistry 41, 2214-2221.

484 Wilcke, W., 2007. Global patterns of polycyclic aromatic hydrocarbons (PAHs) in soil. Geoderma 141, 157-166.

485 Wu, Y., Lin, X., Zhu, Q., Zeng, J., Ding, Q., 2016a. Polycyclic aromatic hydrocarbons (PAHs) pollution and their effects
486 on bacterial community in agricultural soils near a smelting plant. Asian Journal of Ecotoxicology 11, 484-491.

487 Wu, Y., Luo, Y., Zou, D., Ni, J., Liu, W., Teng, Y., Li, Z., 2008a. Bioremediation of polycyclic aromatic hydrocarbons
488 contaminated soil with Monilinia sp.: degradation and microbial community analysis. Biodegradation 19, 247-257.

489 Wu, Y., Tan, L., Liu, W., Wang, B., Wang, J., Cai, Y., Lin, X., 2015. Profiling bacterial diversity in a limestone cave of the
490 western Loess Plateau of China. Frontiers in Microbiology 6.

491 Wu, Y., Teng, Y., Li, Z., Liao, X., Luo, Y., 2008b. Potential role of polycyclic aromatic hydrocarbons (PAHs) oxidation
492 by fungal laccase in the remediation of an aged contaminated soil. Soil Biology and Biochemistry 40, 789-796.

493 Wu, Y., Zhu, Q., Zeng, J., Ding, Q., Gong, Y., Xing, P., Lin, X., 2016b. Effects of pH and polycyclic aromatic
494 hydrocarbon pollution on thaumarchaeotal community in agricultural soils. Journal of Soils and Sediments 16,
495 1960-1969.

496 Zhang, Y., Tao, S., 2009. Global atmospheric emission inventory of polycyclic aromatic hydrocarbons (PAHs) for 2004.
497 Atmospheric Environment 43, 812-819.

498 Zhu, L., Zhang, M., 2008. Effect of rhamnolipids on the uptake of PAHs by ryegrass. Environmental Pollution 156,
499 46-52.

500

Table

Table 1. Experimental treatments in the pot experiment

Treatment	Ryegrass (P)	Lignin (L)	Rhamnolipid (R)
Control	–	–	–
P	+	–	–
L	–	+	–
R	–	–	+
PL	+	+	–
PR	+	–	+
PLR	+	+	+

505 Table 2 Selected parameters for each microbial network in the pot experiment

Network	Nodes	Diameter	Average neighbors	Clustering coefficient	Characteristics Path length
Control	333	16	6.48	0.344	4.99
P	332	20	5.69	0.312	5.70
L	343	13	6.77	0.367	5.09
R	327	15	5.62	0.325	5.17
PL	336	13	12.8	0.419	4.07
PR	320	14	8.93	0.342	3.99
PLR	330	12	11.1	0.400	3.83

506

507

508 **Figure captions**

509 Figure 1. Residuals of the sum of (A) the 15 EPA PAHs and (B) benz(a)anthracene compared to the
510 values before remediation. The results represent the mean ± SD of four replicate pots. Bars
511 with the same letter on top were not significantly different ($p > 0.05$, ANOVA).

512 Figure 2. Shoot and root biomass (A), PAH concentration (B) and calculated PAH amounts (C) in
513 shoots and roots of ryegrass. The values represent the mean ± SD of four replicate pots.
514 Bars with the same lowercase or uppercase letter on top were not significantly different ($p >$
515 0.05, ANOVA). Asterisks indicate a significant ($p < 0.05$ (∗) or 0.01 (∗∗), student's *t*-test)
516 difference between shoot and root.

517 Figure 3. PAH compositions in the original soil, shoots and roots of ryegrass after 90 day cultivation.
518 The values represent the mean ± SD of four replicate pots.

519 Figure 4. Abundances of bacterial 16S rRNA (A), fungal 18S rRNA (B) and Gram positive
520 PAH-RHDα genes (C). The values represent the mean ± SD of four replicate pots, and bars
521 with the same lowercase letter on top were not significantly different ($p > 0.05$, ANOVA).

522 Figure 5. Nonmetric multidimensional scaling (NMDS) analysis of bacterial (A) and fungal (B)
523 communities with OTUs classified at a 97% sequence similarity. The dashed lines separate
524 the lignin-amended treatments from other treatments.

525 Figure 6. Mineralization during the incubation (A) and distribution at the end of the incubation (B) of
526 the ^{14}C radiolabel of [7,12-^{14}C]-BaA spiked to soil microcosms. The values represent the
527 mean ± SD of three replicate microcosms, and bars with the same lowercase letter on top
528 were not significantly different ($p > 0.05$, ANOVA).

Figure 1

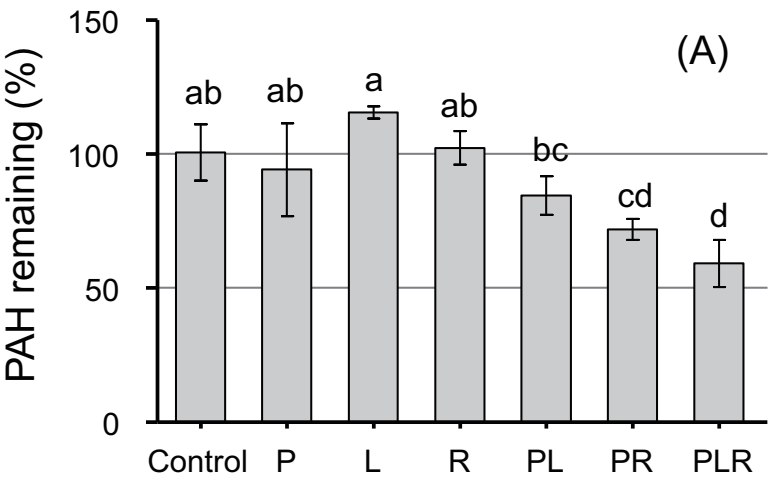
150
100
50
0
PAH remaining (%)
(A)
ab
ab
a
ab
bc
cd
d
Control
P
L
R
PL
PR
PLR

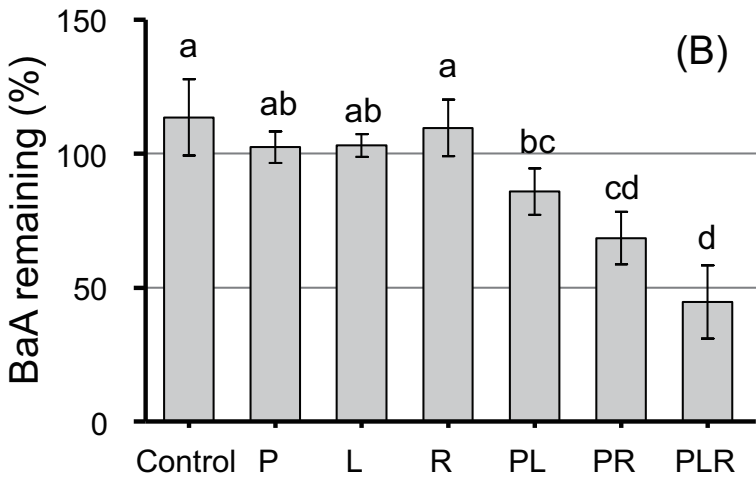
150
100
50
0
BaA remaining (%)
(B)
a
ab
ab
a
bc
cd
d
Control
P
L
R
PL
PR
PLR

Figure 2

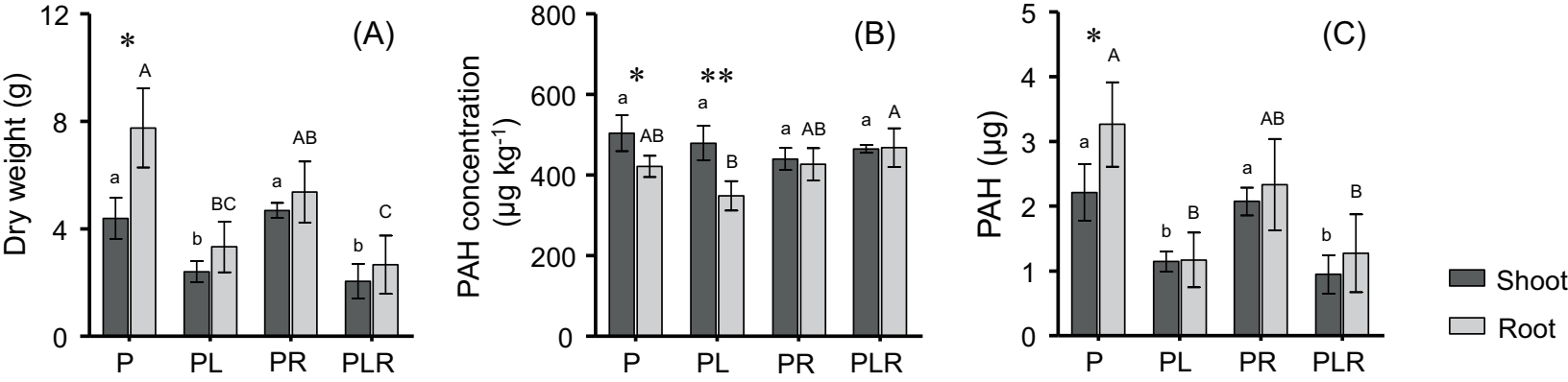
(A)
Dry weight (g)
12
8
4
0
*
a
A
b
BC
a
AB
b
C
P
PL
PR
PLR
(B)
PAH concentration (µg kg-1)
800
600
400
200
0
*
a
AB
**
a
B
a
AB
a
A
(C)
PAH (µg)
5
4
3
2
1
0
*
a
A
b
B
a
AB
b
B
Shoot
Root

Figure 3

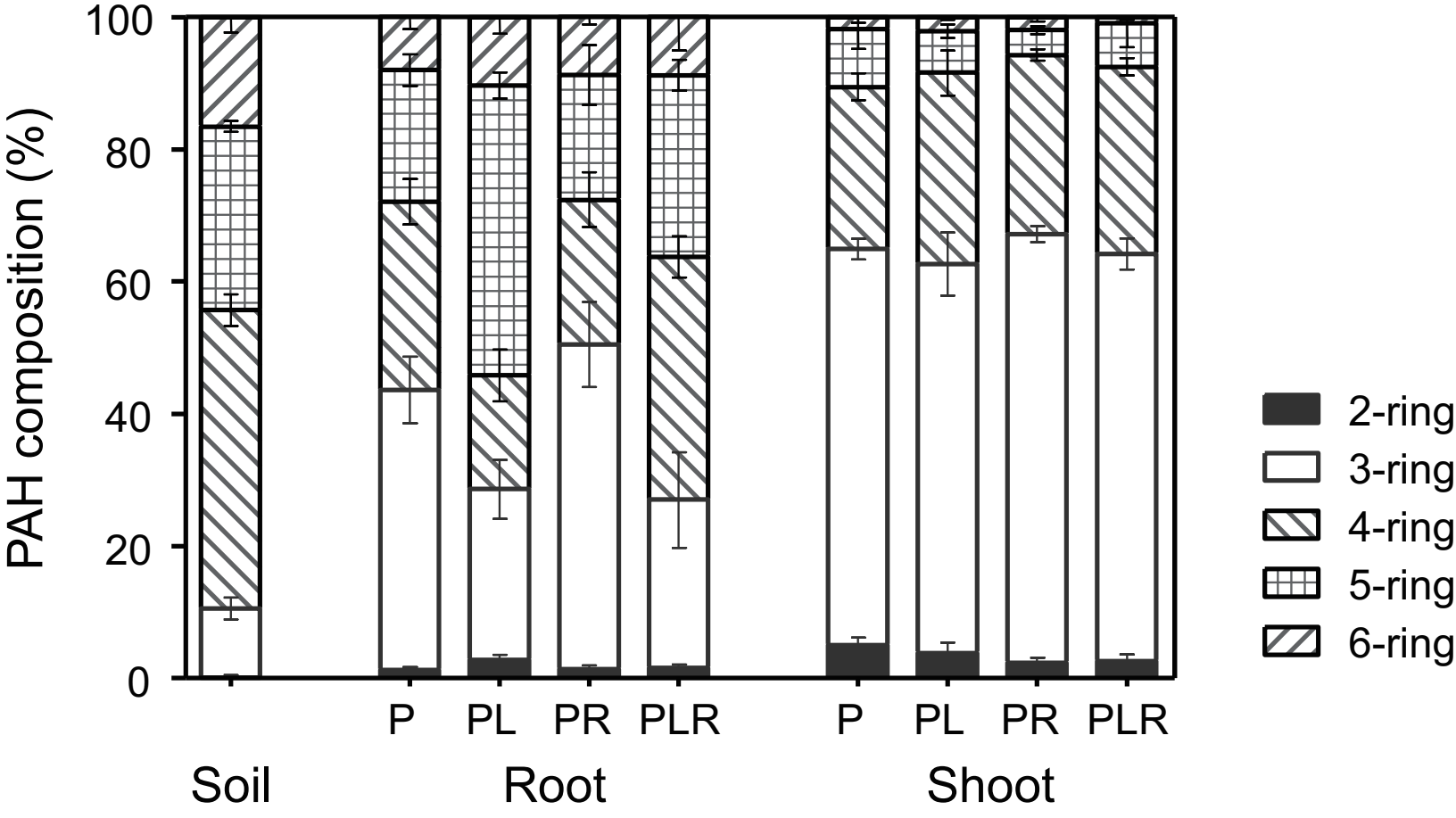
PAH composition (%)
100
80
60
40
20
0
P
PL
PR
PLR
P
PL
PR
PLR
Soil
Root
Shoot
2-ring
3-ring
4-ring
5-ring
6-ring

Figure 4

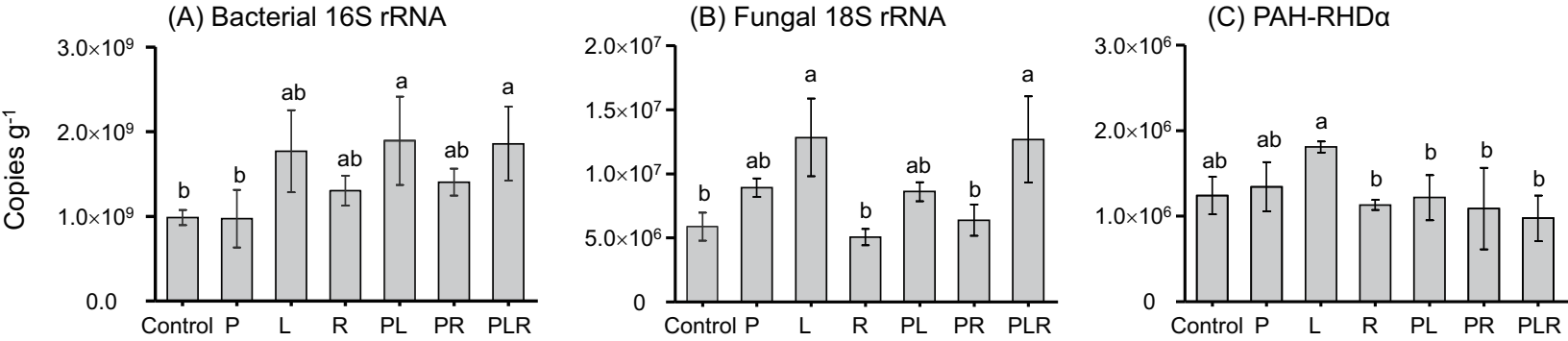
(A) Bacterial 16S rRNA
(B) Fungal 18S rRNA
(C) PAH-RHDα
Copies g-1
3.0×10^9
2.0×10^9
1.0×10^9
0.0
2.0×10^7
1.5×10^7
1.0×10^7
5.0×10^6
0
3.0×10^6
2.0×10^6
1.0×10^6
0
b
b
ab
ab
a
ab
a
b
ab
a
b
ab
b
a
ab
ab
a
b
b
b
Control
P
L
R
PL
PR
PLR

Figure 5

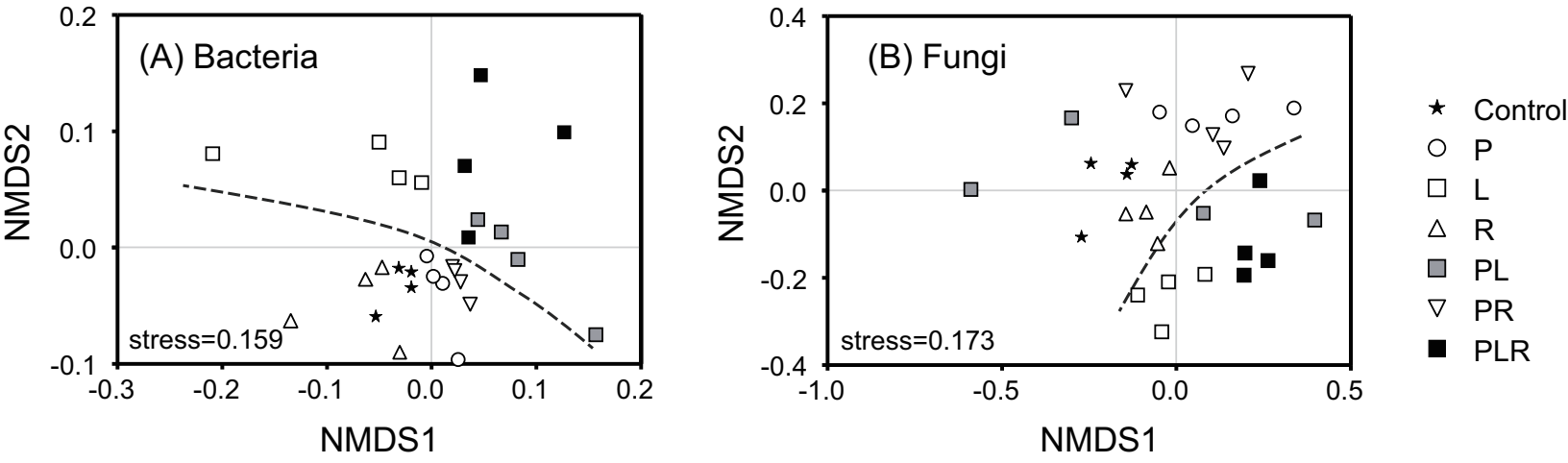
(A) Bacteria
stress=0.159
NMDS1
NMDS2
0.2
0.1
0.0
-0.1
-0.3
-0.2
-0.1
0.0
0.1
0.2
(B) Fungi
stress=0.173
NMDS1
NMDS2
0.4
0.2
0.0
-0.2
-0.4
-1.0
-0.5
0.0
0.5
Control
P
L
R
PL
PR
PLR

Figure 6

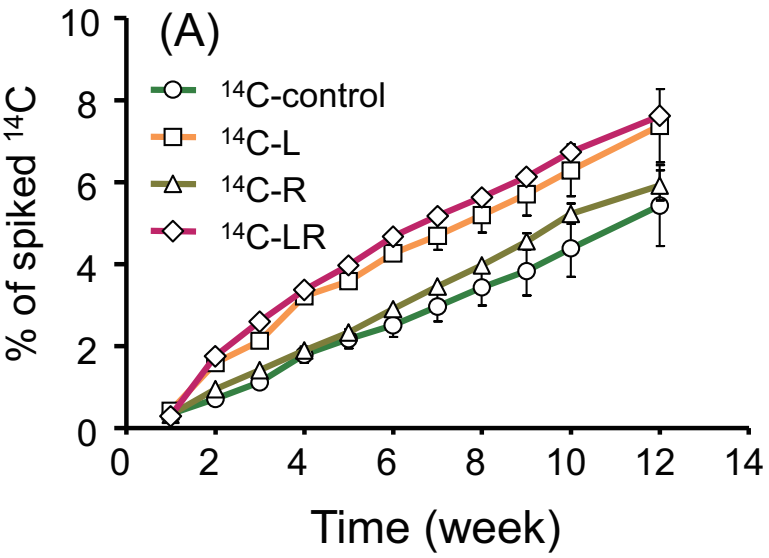
(A)
% of spiked 14C
Time (week)
14C-control
14C-L
14C-R
14C-LR
0
2
4
6
8
10
12
14

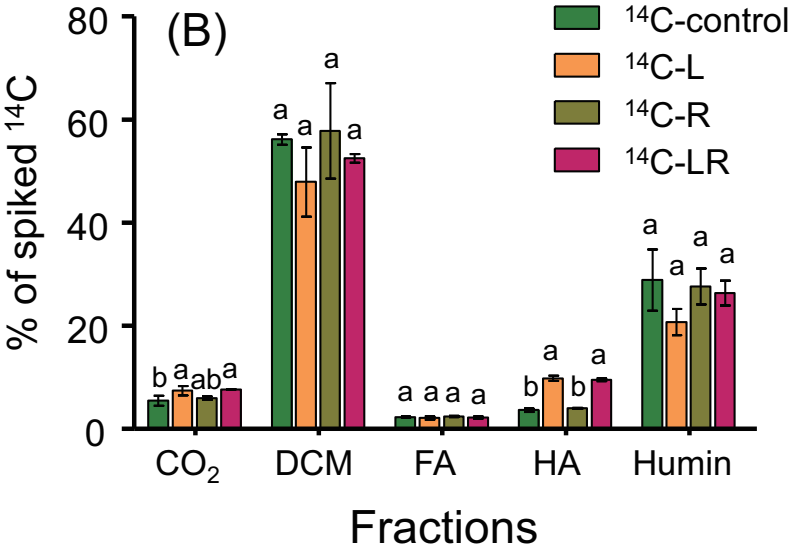
(B)
% of spiked 14C
Fractions
14C-control
14C-L
14C-R
14C-LR
CO2
DCM
FA
HA
Humin
0
20
40
60
80

Supplementary figures

Click here to download Supplementary Material for online publication only: Supplementary materials.docx